Carbon – Science and Technology

ISSN 0974 – 0546

http://www.applied-science-innovations.com

ARTICLE Received : 01/03/2009, Accepted : 14/04/2009

# Removal of cationic surfactant (CTAB) from aqueous solution on to activated carbon obtained from corncob

**S. M. Yakout and A. A. Nayl**

*Hot Lab. Centre, Atomic Energy Authority, Cairo, Egypt.*

***Direct and indirect releases of large quantities of surfactants to the environment may result in serious health and environmental problems. Therefore, surfactants should be removed from water before water is released to the environment or delivered for public use. Using powdered activated carbon (PAC) as adsorbent may be an effective technique to remove surfactants. In this study, the removal of surfactants by PAC was investigated and the influences of the operating parameters on the effectiveness on adsorption rate were studied. Cationic surfactant, Cetyl trimethyl ammonium bromide (CTAB) was selected for the experiments. A series of batch experiments were performed to determine the sorption isotherms of surfactants to PAC. The results showed that carbon structure affect mainly on the surfactant adsorption. Surfactant equilibrium data fitted very well to the binary langmuir model. The pseudo first-, second- order and intraparticle diffusion kinetic models were applied. Both, the external mass transfer and intraparticle diffusion mechanisms involve in CTAB sorption.***

## 1. Introduction :

Surface-active agents, or surfactants, are widely used in many industrial and commercial products and processes throughout the world. Surfactants are not only related to soaps and detergents in daily life, they are also in heavy demand for industrial processes requiring colloid stability, metal treatments, mineral flotation, pesticides, oil production, pharmaceutical formulation, emulsion polymerization, and particle growth [1, 2]. The broad range of surfactant applications may also cause side effects in the environment and in these industrial processes. The application of surfactants can also produce environmental pollution and raises a series of problems for wastewater treatment plants [3].

One of the common methods to remove surfactants from water is to use adsorption technology. Surfactant adsorption has been studied extensively. Additionally, several materials have been investigated as surfactant adsorbents. These include layered double hydroxides [1, 4], zeolites [4, 5], silica [6], mineral oxides (alumina) [1, 4, 7 – 9], polymers [10], natural and synthetic fibers [11], and activated carbons (ACs) [5]. Different adsorption mechanisms and models have been proposed, depending on the adsorbent–adsorbate system. Activated carbons are used as adsorbent in many industrial applications as economic mass separation agent to raise the final product quality. Drinking water, wastewater treatment processes, food and chemical industry processes are typical examples [12 – 15]. More recently, ACs are increasingly used as adsorbents for the purification of process streams within industrial chemical processes, again owing to their high adsorption efficiency [16]. As mass separation agents, ACs, present useful physical and chemical properties. These include high specific surface areas, wide pore size distributions (including micropores and mesopores) [14, 15, 17 – 22], hydrophobic surfaces [23], and variable surface functional groups [17, 22, 24]. Each property supports the application of ACs as adsorbents for surfactant concentration reduction or removal.

Most commercially available ACs are generated from low cost materials of high carbon content, such as coconut shells, agricultural waste, coal, and wood. From the adsorption experimental point of view, the relatively hydrophobic character and high specific gravity of ACs makes their separation from the solution phase a simple operation [17]. The physical properties of ACs mentioned above, as well as their relatively inexpensive availability, make them suitable for use as adsorbents in large-scale continuous processes. In these studies, the sorption of organics onto PAC was the main focus which shows quite different characteristics (i.e. micelle formation) than the other organic pollutants. The specific objective of this study is to explore the removal of surfactants by PAC, and to determine the influence of the operating parameters on its removal effectiveness. A cationic surfactant (CTAB) was selected for the experiments. First, a series of batch experiments were performed to identify the adsorption kinetics of CTAB, determine the sorption isotherms of

surfactants. Influences of activated carbon characterization and concentration on surfactant adsorption were investigated.

## 2. Materials and Methods :

### 2.1 Activated Carbon Samples :

Corncobs are yearly generated in Egypt as an agricultural by-product. In this study, activated carbon was prepared using two-step process described elsewhere [25] : corncob was first carbonized into char. The char was soaked in a concentrated NaOH solution, oven-dried, and then activated.

Corncobs were dried at 110 ◦C for 24 h, placed in column-typed stainless steel tube, and heated at a rate of 30 ◦C/min from room temperature to 450 ◦C. In the meantime, $N_2$ was poured into the oven at a rate of 80 ml/min. Under such oxygen-deficient conditions, corncobs were thermally decomposed to porous carbonaceous materials and hydrocarbon compounds. This is the carbonization step.

After the carbonization step, a char/corncob ratio of 35.7 % was obtained. The chars were removed and crushed. These powders were well mixed with water and KOH in a stainless steel beaker with the weight ratio of KOH / char equal to 3. Water was evaporated at 130 ◦C for 24 h, and these dried mixtures consisting of chars and KOH (without KOH lost) was obtained. The dried mixtures were placed in column tube oven, heated to 850 ◦C, and kept at this temperature for 1.2 h. In the meantime, nitrogen gas was flowed into the oven at a rate of 80 ml/min. The activated products were cooled to room temperature and washed with deionized water. These samples were poured to a beaker containing 0.1 mol HCl (250 $cm^3$) and stirred for 1 h. Finally, they were washed with hot water until pH of the washing solution reached ca. 6 – 7. The dried powders were sieved in the size ranged from 0.177 to 0.42 mm. The sample activated by this method labeled as Cob850 and original corn cob sample was labeled as Cob0. The same procedure was repeated except that activation occur in aluminum foil cover, this sample was labeled as Cob850/Al

The BET surface area of carbons was obtained from the $N_2$ adsorption isotherm at 77 K on an automatic adsorption instrument (Quantachrome Instruments, Model Nova1000e series, USA). Prior to this measurement, the samples were first dried in an oven at 130 ◦C overnight and then, quickly placed into the sample tube. After that, the tube was heated to 230 ◦C and evacuated for 4 h until the pressure was less than $10^{-4}$ Torr. The total pore volume (Vpore) was reduced from the adsorption data based on the manufacturer's software and the pore size distribution was derived from the The Dubinin - Astakhov theory [26]. The micropore volume (Vmicro) were deduced using the t -plot method [27].

### 2.2 Surfactants :

The cationic surfactants utilized in this work contained a quaternary ammonium functional group, which is comprised of a positively charged central nitrogen atom with 4 bonds to carbon atoms. Cetyl trimethyl ammonium bromide, CTAB, ($C_{19}H_{42}NBr$) was selected as a cationic surfactant. CTAB was obtained from Fluka at 98 % purity and was used as received. The critical micelle concentration CMC of CTAB was reported as 0.92 mM 25 °C (28). Water for solutions was distilled and deionized (Milli-Q Plus, Millipore).

### 2.3. Batch adsorption experiments :

Sorption of CTAB to AC was investigated at varying concentrations above and below CMCs using 100 mL of glass flasks. A solution of 100 mL was added to each flask and equilibrated with 0.1 g of AC for 120 min at 25 °C. Just prior to use, adsorbents were dried in an oven at 110 °C for 24 h and kept in a desiccator until the samples reached room temperature. Flasks were placed in an air shaker, at room temperature until adsorption equilibrium was reached. After equilibrium, solid liquid mixture was separated by filtration (0.45 mm Whatman Filter Paper). It was found that the surfactant sorption to filter paper was insignificant. Following filtration, CTAB were analyzed using UV (UV-160A SHIMADZU).

The adsorption isotherms of surfactants were determined on the basis of batch analysis. The ACC pieces of varying masses were allowed to equilibrate with solutions of surfactants in water, with known initial concentrations at 25 °C for 3 h. The concentrations at the end of equilibration period were measured spectrophotometrically. The amount of surfactant adsorbed per unit mass of the ACC at equilibrium, qe, was calculated by Equation (1) :

$$q_e = \frac{\nu(C_0 - C_e)}{m} \quad \text{.....(1)}$$

where ν is the volume of the solution of surfactant (L), $C_0$ and $C_e$ are the initial and equilibrium concentrations, respectively (mM) and m is the mass of the AC (g). Then Equation (1) gives qe in mmol surfactant adsorbed per gram AC.

## 3. Results and Discussion :

Correctly interpreting surfactant adsorption in an aqueous solution is a complex and challenging procedure. The multi-component nature of the adsorptive system leads to complex interactions between the surfactant adsorptive and the AC adsorbent. Various mechanisms are involved [4]. The physical and chemical characteristics of each AC also affect surfactant adsorption. To present a systematic analysis of the surfactant–AC system, we begin by addressing the influence of the solvent conditions on AC physical and chemical properties. Once these details are established, we define the adsorption isotherms and interpret the amount adsorbed in terms of the adsorbent properties and in terms of the solution properties, from which we propose a systematically derived, qualitative mechanism for CTAB adsorption.

### 3.1. Activated Carbon Characterization :

The properties of the adsorbents (Cob850, Cob850/Al, and Cob0) were characterized in terms of pore volume, surface

area and pore size distribution and these properties were correlated to the surfactant adsorption capacity. The resulting characteristics determined by $N_2$ gas adsorption at 77 K are illustrated in Table (1). The data obtained shows that carbon Cob850 offers the highest micropore volume, original Cob0 carbon the least, and Cob850/Al carbon an intermediate volume. Also, the order of the total pore volume is Cob850 > Cob850/Al > Cob0. The data in Table (1) also suggest that the mesopore volume of activated carbon sample Cob850 is negligible compared with its total pore volume in verse of Cob850/Al sample.

Table (1) : Pore characteristics of carbon samples.

| Parameter | CC original | CC850/Al | CC850 |
|---|---|---|---|
| BET surface area $nm^2/g$ | 0.3 | 23.9 | 1203.6 |
| Total pore volume cc/g | 0.003 | 0.016 | 0.541 |
| Micro pore volume cc/g | 0.001 | 0.007 | 0.486 |
| Meso pore volume cc/g | -* | 0.01 | 0.0549 |
| Average pore Radius nm | -* | 1.34855 | 0.89888 |

* These value not determined due to its low values.

It is apparent that all isotherms of all carbon series (Figure 1) belonging to type I and IV, according to BDDT classification with an hysteresis loop typical of micropores for Cob850 carbon sample and mesopores for Cob850/Al sample (29). This indicate that Cob850 carbon sample is mainly micropores with great surface area and total pore volume while Cob850/Al sample is mainly mesoporous material with low surface area

The overall changes for sample Cob850 and Cob850/Al suggest that activation in the absence of aluminum foil more effective on the pore characteristics. The increased pore volume compared to original corn cob suggests that either some new micro pores or meso pores were formed during the caustic treatment or some carbonaceous material or functional groups initially blocking the entrance to some mesopores may be removed during the strong caustic treatment. Therefore, KOH played a decisive role for the formation of pores. Following reactions may take place during the activated processes under high temperature **[30]**

$$2KOH \rightarrow K_2O + H_2O \quad \text{..... ..... (2)}$$

$$C + H_2O \rightarrow H_2 + CO \quad \text{..... ..... ...(3)}$$

$$CO + H_2O \rightarrow H_2 + CO_2 \quad \text{..... ..... ...(4)}$$

$$K_2O + CO_2 \rightarrow K_2CO_3 \quad \text{..... ..... ...(5)}$$

$$K_2O + H_2 \rightarrow 2K + H_2O \quad \text{..... ..... ...(6)}$$

$$K_2O + C \rightarrow 2K + CO \quad \text{..... ..... ...(7)}$$

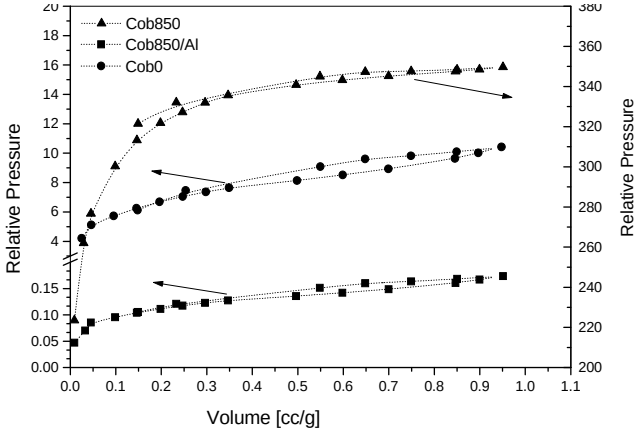


Figure (1) : Nitrogen adsorption isotherms for all carbon samples.

Recently, Dubinin A ask our method of micropore width distribution analyses for these carbon samples shown in Figure (2) exhibits a relative widening of the width distribution, accompanied by a modest decrease in the relative volume adsorbed with pore width **[31]**.

From Figure (2), it is clear that the samples exhibit narrow pore size distribution, with peak in oscillate in region of 0.8 to 1.0 nm. The results illustrate that activation method appears to affect pore size distribution, Cob850 carbon have pore volume highly greater than Cob850/Al and Cob0.

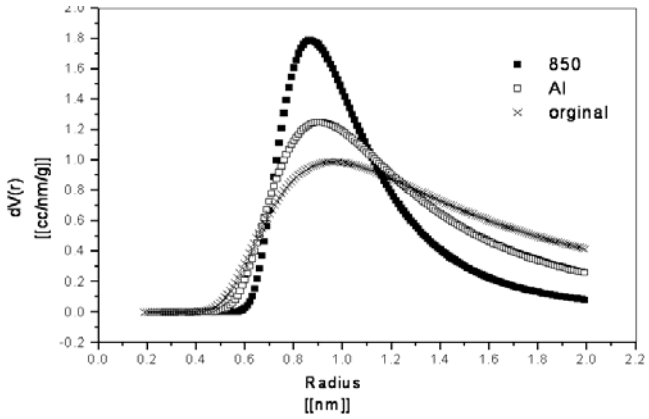


Figure (2) : Pore size distribution of activated carbon samples.

## 3.2. Variation of activation on surfactants adsorption :

The variation of adsorbent that include raw corn cubs before and after activation, at fixed dose of adsorbate, with constant concentration of surfactant with optimum contact time, (Table 2). Adsorption increased after activation may be attributed to increase in availability of the active sites due to this increase in surface area and internal volume and a larger pore size especially in case of cob850 sample which was selected for further woke.

Table (2) : Variation of activation on CTAB surfactants adsorption onto Cob850 carbon.

| Adsorbent | Uptake (Mm/g) |
|---|---|
| Cob0 | 1.6 |
| Cob850/Al | 9.0 |
| Cob850 | 25.3 |

**3.2.1. Effect of adsorbent mass** :

The effect of adsorbent mass (Cob850) on amount of surfactant adsorbed was undertaken with a fixed surfactant concentration (1.0 Mm) and contact time (one hour) by varying the mass of adsorbent. This study reveals that amount of surfactant adsorbed exponentially decreases with increase in Cob850 mass (Figure 3) and reached to constant removal value after a particular carbon concentration (50 mg) beyond which there is no significant decrease in surfactant uptake. This behavior may be due to as the dosage of adsorbent increased, the adsorption sites remain unsaturated during the adsorption reaction leading to drop in adsorption capacity or due to aggregation/agglomeration of sorbent particles at higher concentrations, which would lead to a decrease in the surface area and an increase in the diffusional path length. The particle interaction at higher adsorbent concentration may also help to desorbs some of the loosely bound anions from the sorbent surface [32].

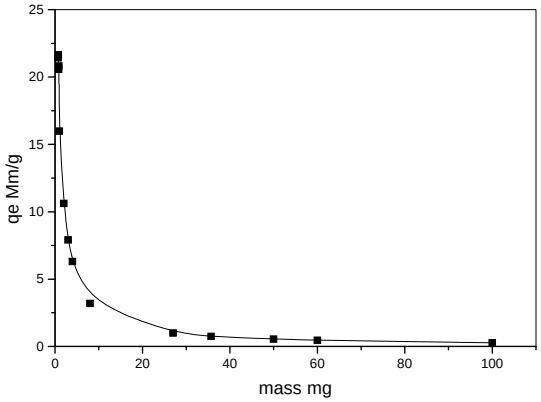


Figure (3) : Effect of Cob850 carbon mass on CTAB surfactant uptake ($q_e$).

## 3.2.2. Effect of contact time :

In adsorption studies, effect of contact time plays vital role irrespective of the other experimental parameters effecting adsorption kinetics. The adsorption studies were carried out at different contact time as constant initial concentration of adsorbate with fixed dose of Cob850 carbon (Figure 4). It is observed that at initial stage, adsorption is rapid then becomes slow and gets stagnated with increase in time. There seems to the time variations on extent of adsorption can be divided into three different regimes, they are : (1) linear increase in adsorption with time, (2) transition regime where the rate of adsorption levels off and (3) a plateau regime. The range over which the regions extend varies with the bulk concentration, nature of surfactant, and so on. The nature of solid surface, that is the hydrophobic or hydrophilic, and the electrical interactions play an important role in the kinetics of adsorption of surfactant at the solid–liquid interface. Adsorption kinetics of cationic surfactant on Cob850 carbon shows that the total equilibrium time is approximately 40–50 min and at least 90 % adsorption was complete within 10 min. then one hour was sufficient for complete adsorption. This time was taken for further work.

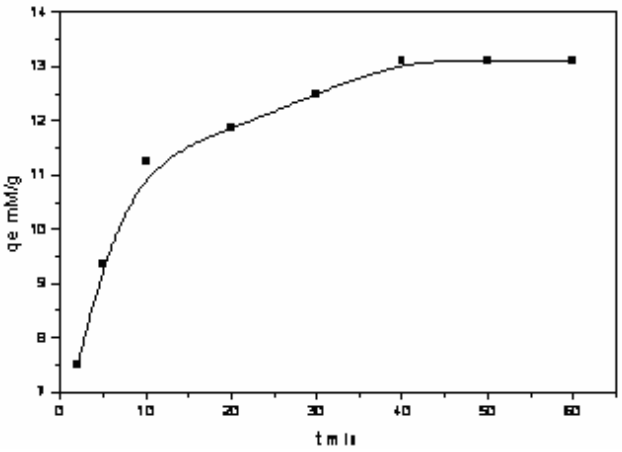


Figure (4) : Effect of time on adsorption of CTAB on Cob850 carbon.

## 3.2.3. Surfactant adsorption kinetics :

The kinetics of surfactant adsorption is a fundamental problem of interfacial science playing a key role in various processes and phenomena, such as wetting, foaming and stabilization of liquid films [33, 34]. The study of sorption kinetics in wastewater treatment is significant as it provides valuable insights into the reaction pathways and into the mechanism of sorption reactions due to the fact that as it was based on the process kinetics reaction mechanisms may be hypothesized. Therefore, it is important to be able to predict the rate at which pollutant is removed from aqueous solutions in order to design appropriate sorption treatment plants.

Three kinetic models, i.e. the first-order equation, the pseudosecond-order equation and an intraparticle diffusion equation, were considered for interpreting the experimental data [34].

The first-order rate expression (Lagergren equation) is given as :

$$\log(q_e - q_t) = \log q_e - \frac{k_1}{2.303} t \qquad ....(8)$$

The pseudo-second-order kinetic model [28] is expressed as

$$\frac{t}{q_t} = \frac{1}{k_2 q_e^2} + \frac{t}{q_e} \qquad .....2nd\ order\ (9)$$

The intraparticle diffusion equation [35] can be written by following :

$$q_t = k_p t^{0.5} \qquad \text{.....(10)}$$

where $q_e$ and $q_t$ are the amounts of surfactant adsorbed on adsorbent at equilibrium and at various times t (mmol $g^{-1}$); $k_1$, the rate constant of the first-order model for the adsorption process ($min^{-1}$); $q^2$, the maximum adsorption capacity (mmol $g^{-1}$) for the pseudo-second-order adsorption; $k_2$, the rate constant of the pseudo-second-order model for the adsorption process (g $mmol^{-1}$ $min^{-1}$); $k_p$, the intraparticle diffusion rate constant (mmol $g^{-1}$ $min^{-1/2}$). $k_1$ can be obtained from the straight line of plot $\log(q_e-q_t)$ vs. t from Equation (8) and $k_2$ from Plot of t vs. $t/q_t$ from Equation (9), The $k_p$ is the slope of straight-line portions of plot of $q_t$ vs. $t^{0.5}$ from Equation (10).

The results of the kinetic plots were shown in Figure (5 and 6). Table (3) lists the calculated results of the kinetic parameters $k_1$, $k_2$, $q_{e,calc}$, and the initial adsorption rate h ($=k_2 q_e^2$) along with the corresponding correlation coefficients.

As can be seen from Table (3), the equilibrium sorption capacities and correlation coefficients $r^2$ for second order model are much more reasonable when compared with experimental results than those of the first-order system. Since most of the first-order $q_{e,calc}$ (19.3 mmol/g) values deviate significantly from the experimental values (13.6 mmol/g) it suggests that the sorption of CTAB onto Cob850 follows the pseudo-second-order model. Further, there was very minor deviation between expected and observed $q_{e,calc}$ (amount of CTAB adsorbed at equilibrium, mmol/g) values. It can be said that more than one-step may be involved in sorption process.

The higher rates and extents of adsorption of CTAB can be attributed to the presence of hydrophobic long chain hydrocarbons in the structures of the molecules. This shows that predominant interaction between the surface and the surfactants is hydrophobic in water solutions. The pH of these adsorbate solutions in water is around 6, close to the $pH_{PZC}$ of the Cob850 carbon surface. Therefore, although we cannot exclude the electrostatic interactions, they are of secondary importance compared to hydrophobic interactions in adsorption from $H_2O$ solutions.

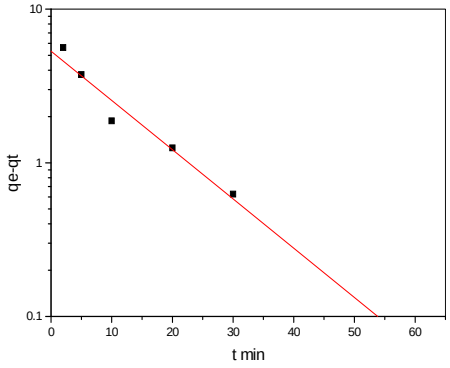


Figure (5) : Pseudo-first-order sorption kinetics of CTAB on Cob850 carbon.

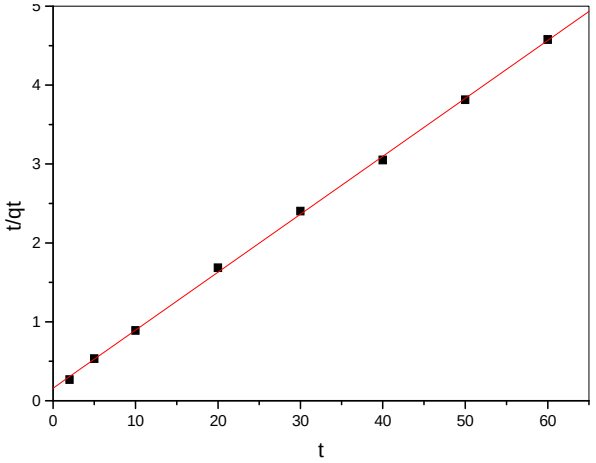


Figure (6) : Pseudo-second-order sorption kinetics of CTAB on Cob850 carbon.

Sorption kinetic data was further processed to determine whether intraparticle diffusion is rate limiting and to find the rate parameter for intraparticle diffusion ($k_p$). CTAB uptake against square root of contact time ($t^{0.5}$) is shown in Figure (7).

The multi-linearity appearing in Figure (7) indicates that two or more phenomena occur successively. The first, stage is the external surface adsorption or instantaneous adsorption stage. The second, gradual linear stage is the gradual adsorption stage, where intraparticle diffusion is the controlling factor of the adsorption process. The third, linear stage is the final equilibrium stage where the intraparticle diffusion starts to slow down because of extremely low solute concentration in the solution. Since activated carbon consists of a network of interconnected pores of varying sizes which are classified according to their diameter; micropores < 2.0 nm, mesopores 2 – 50 nm and macropores > 50.0 nm, the pores provide a large internal surface area, the behavior of multilinearity may also attributed to diffusion in pores with different sizes.

As shown in Figure (7), the instantaneous adsorption in the first stage is not absent in the working range and completed within about 3 min. The second stage due to intraparticle diffusion, being rate-controlled, is immediately attained at the beginning (nearly in 3 min) of the adsorption process. The third section is due to a drop in diffusion rate. That is, final equilibrium stage is nearly attained. In other words, the CTAB molecules are slowly transported via intraparticle diffusion into the particles and are finally retained in micropores. A good correlation of rate data with the linearized form of the model indicates that diffusion mechanisms control the rates. In general, the slope of the lines in each stage is called the rate parameter $k_p$. Table (3) presents intraparticle diffusion constants ($k_{p,1}$, $k_{p,2}$). The $k_{p,1}$ and $k_{p,2}$ express intraparticle diffusion rates of the first and second stages in the adsorption **[36]**.

From Table (3), it is seen that the order of adsorption rate was the first stage ($k_{p,1}$) > second stage ($k_{p,2}$). It can be concluded that CTAB was adsorbed by the exterior surface of AC particle at the beginning, so the adsorption rate was very fast. When the adsorption of the exterior surface

reached saturation, the CTAB entered into PAC particle by the pore within the particle and was adsorbed by the interior surface of the particle. When the CTAB diffused in the pore of the particle, the diffusion resistance increased, which caused the diffusion rate to decrease. With decrease of the CTAB concentration in the solution, the diffusion rate became lower and lower and the diffusion processes reached the final equilibrium stage. Therefore, the changes $k_{p,1}$, and $k_{p,2}$ could be attributed to the adsorption stages of the exterior surface, interior surface and equilibrium, respectively **[37]**

Table (3) : Adsorption kinetic parameters of CTAB adsorption onto Cob850 carbon

| Model | Parameter | |
|---|---|---|
| *First-order model* | $q_{e,exp}$ (mmol/g) | 13.1 |
| | $K_1$ ($min^{-1}$) | 0.22 |
| | $q_{e,cal}$ (mmol/g) | 19.3 |
| | $R^2$ | 0.92 |
| *Second-order model* | ***$K_2$ (g/mmol min)*** | 0.033 |
| | h (mmol/g min) | 6.21 |
| | $q_{e,cal}$ (mmol/g) | 13.6 |
| | $R^2$ | 0.999 |
| *Intraparticle diffusion model* | $Kp_1$(1st stage) | 2.14054 |
| | $R^2$ | 0.994 |
| | intercept | 4.5 |
| | $Kp_2$(2nd stage) | 0.58926 |
| | $R^2$ | 0.995 |
| | Intercept | 9.31208 |

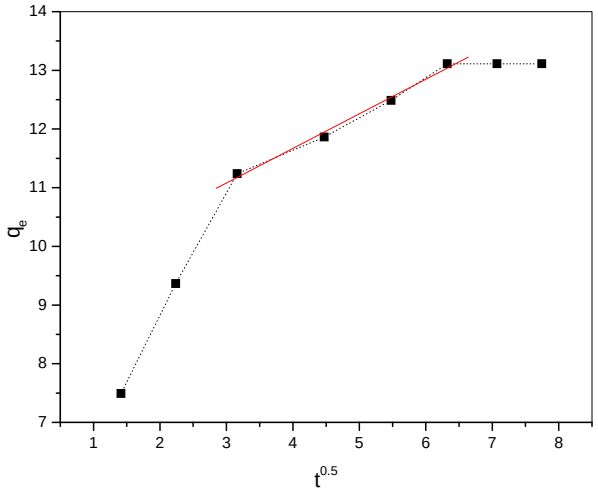


Figure (7) : Intra-particle Diffusion plots for adsorption of CTAB on Cob850 carbon.

**3.3. Equilibrium adsorption of surfactant :**

The equilibrium adsorption isotherms for CTAB to Cob850 are presented in Figure (8). The results showed that CTAB sorption to Cob850 occurred in four steps. In general, a typical isotherm can be subdivided into four regions when plotted on a log–log scale (Figure 9) **[38].**

Region (I) adsorption occurs at low equilibrium surfactant concentrations and is known as Henry's law adsorption region. The surfactant molecules adsorb individually and linearly in this region with minimal lateral interactions between adsorbed surfactants **[39]**. With increasing surfactant concentration, the slope of the adsorption isotherm increases sharply at the critical admicelle concentration, which marks the onset of Region (II) adsorption. Region (II) shows a sudden increase in the adsorption due to lateral interaction between the adsorbed monomer, resulting surface aggregation of the surfactants. Region (III) is characterized by a decrease in isotherm slope relative to the slope in Region (II). This change in slope can be attributed to lateral electrostatic repulsion between surfactant molecules and/or surface site heterogeneities.

Region (IV) is the plateau adsorption region, which commences at the CMC (0.92 mM) of the surfactant system. At the CMC, the concentration of the surfactant monomer becomes constant and consequently no further adsorption occurs at higher surfactant concentrations. It should be noted that this plateau adsorption may not reflect complete surface bilayer coverage.

Therefore, it would be reasonable to assume that the rising part in the adsorption isotherms indicates that adsorbate–adsorbate interactions at the solid–liquid interface take place. Then, two adsorption mechanisms could be adopted to explain the whole adsorption process of CTAB surfactants on the carbon surface, i.e. monolayer adsorption followed by surface aggregation **[40]**.

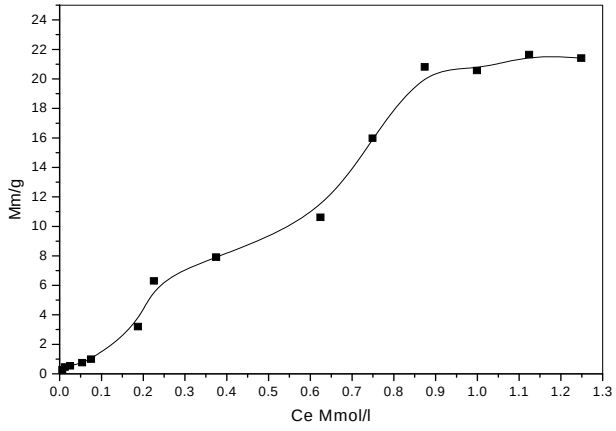


Figure (8) : Equilibrium adsorption isotherm of CTAB on Cob850 carbon.

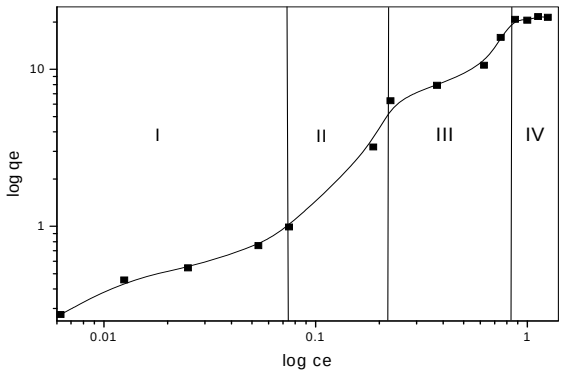


Figure (9) : Schematic presentation of four-regime CTAB adsorption isotherm onto Cob850 carbon.

### 3.4. Isotherm Modeling :

An equation to express the adsorption equilibrium relationship is often needed. This is usually done by fitting experimental data to an isotherm model. Nevertheless, the different kind of interactions that progressively dominates the surfactants adsorption process suggests very unlikely that a single adsorption equation—which comes at the end from an assumed adsorption model dictated by a single kind of interactions—could fit the whole range covered in the isotherm. We will analyze the adsorption behavior with the help of a bi-Langmuir equation, but, as a first step, we have studied the most diluted concentration range (below the c.m.c. of the surfactants) are correlated with the well-known Langmuir model, where it could be expected that there is not interaction among adsorbed molecules and there is a constant average adsorption free energy value so the adsorption mechanism should be dominated near exclusively by one kind of interaction, adsorbate – adsorbent. The Langmuir model was selected because of its simplicity, easy incorporation in future design models and previously demonstrated ability to describe surfactant adsorption **[41]**

$$X = \frac{X_m C b}{1 + C b} \qquad (1)$$

Langmuir equation provides an estimate of the maximum adsorption capacity, assumed as complete monolayer coverage, Xm, and through the parameter b a measure of the adsorbate– adsorbent interaction free energy, $\Delta G_{ads}$:

$$\Delta G_{ads} = -RT \ln(b\omega) \qquad (2)$$

where ω refers to the water concentration in solution (55.55 mol l_1 at 20 8C). R= universal gas constant (1.987 cal/mol K or 8.314 J/mol k) and T is absolute temperature in Kevin (K).

As shown in Figure (10), Langmuir equation matches the experimental results very accurately up to a concentration value around 0.6 mmol/1 below but near the c.m.c. of the surfactants CTAB, after which it gets worse (0.9 mmol). Nevertheless, the curves obtained from this adjustment have been extrapolated for the entire range of concentration studied (Figure 10), shows clearly that contributions due to adsorption mechanisms different than direct adsobate–adsorbent interaction are gaining importance as the concentration increases above c.m.c. **[42]**

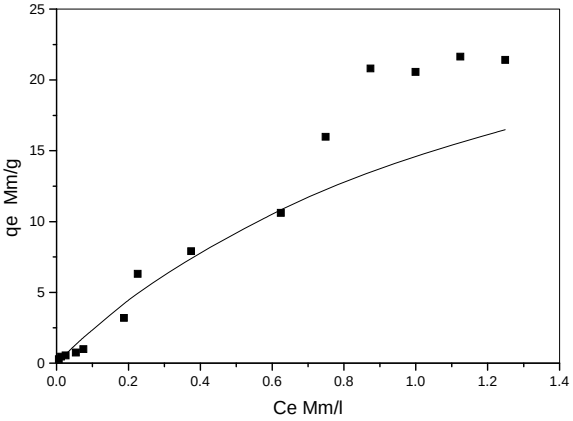


Figure (10) : Fitting of the experimental results of CTAB adsorption onto Cob850 carbon by a simple Langmuir model.

The area per adsorbed CTB molecule, Am, evaluated according to **[42]** :

$$A_m = \frac{S}{X_m N_A} \qquad (3)$$

where S is the accessible surface area of the carbon determined by nitrogen adsorption at 77 K, $S_{N2}$, and $N_A$ is Avogadro's number. The Am values obtained is 0.05 $nm^2$/molecule **[43]** lower than contactable surface area of CTAB molecules evaluated from their molecular dimensions (0.47 $nm^2$). This fact indicates the higher contribution from narrowest pores for CTAB surfactants adsorption.

The large negative values of $\Delta G_{ads}$ indicate strong extent of adsorption of CTAB on the Cob850 surface. This may be due to dispersive interactions between the delocalised π electrons on the surface of the basic activated carbons Cob850 and the free electrons of the CTAB molecule present in the ammonium group and multiple bonds, play a role in the adsorption mechanism· This could be supported by the fact that the adsorption extent was not affected by the change in the pH. The change in the pH modifies the charges on the AC surface, and hence affects the electrostatic interaction between the CTAB and the AC surface. The p–p interaction, however, is not affected by the charge modification on the AC surface and hence is not affected by the change in the pH **[44]**.

As we have previously discussed, we will try to analyze the adsorption behavior with the help of a double scheme of Langmuir. For this purpose, the experimental results of the surfactants adsorption onto the activated carbon for the entire range of C studied were fitted to equation **[42]** :

$$X = \frac{X_{m2} C b_2}{1 + C b_2} + \frac{X_{m3} C b_3}{1 + C b_3} \qquad (4)$$

where the parameters have the habitual meaning of the Langmuir equation. The curves resulting from that fit, curve labeled as 1, have been plotted in Figure (11) together with each of the summed curves (curves 2 and 3); hence, curve 1 is the sum of curve 2 and 3. It can be seen that curve 1 closely matches the experimental dates and that each of the curves 2 and 3 has a similar shape for all the adsorption systems. Curve 3 has a nearly quickly reaches a well-defined plateau. Curve 2 has a small slope at the lowest C, but it changes smoothly with C in the whole range. Thus, the behavior of curve 1 is controlled by curve 3 and 2 at the lowest and the highest concentrations, respectively. This mathematical behavior allows the analysis of the whole CTAB surfactants adsorption onto the activated carbon into two steps: the surfactant adsorption by direct interaction with the carbon surface, which can be assumed as completed when concentration reaches values close to the surfactant c.m.c. (curve 3); and a second process, mainly above the c.m.c., for which the newly adsorbed molecules are retained by interaction with those previously adsorbed (curve 2), both of them described by a Langmuir equation.

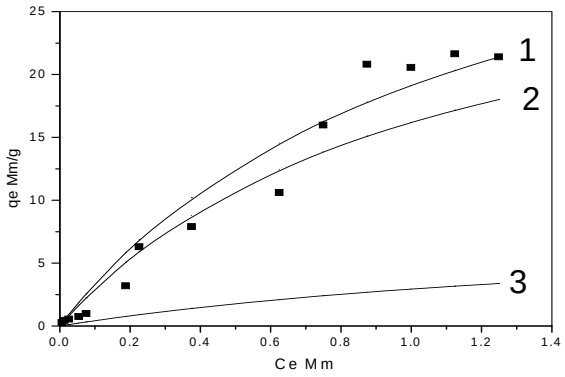


Figure (11) : Fitting of the experimental results of CTAB adsorption onto Cob850 carbon by a double Langmuir scheme (curve 1) and each of the summed curves (curves 2 and 3).

The $X_m$ and b values found from both curves are reported Table (4), with the sub-index representing the curve from which they were obtained. The value of area occupied per molecule in each of the two proposed processes, $A_{m3}$ and $A_{m2}$, and the adsorption free energy, $\Delta G_{ads3}$ and $\Delta G_{ads2}$, as well as their values per molecule, $\Delta g_{ads3}$ and $\Delta g_{ads2}$, are also given in Table (4).

As it was mentioned, at the lowest equilibrium concentrations, the adsorption process takes place by direct adsorbate–adsorbent interactions; this behavior must be manifested in our treatment by the curve representative of such process (curve 3). Xm3 is lower than Xm2, although it can be distinguished important differences related to its relative contribution on curve 1 (Table 4). Also, the values of $\Delta g_{ads3}$ are similar to those calculated from a simple Langmuir equation, $\Delta g_{ads}$ (Table 4), since both are related to the same type of interaction, and they reflect the stronger adsorption of CTAB surfactant. At the lowest equilibrium concentrations, adsorption takes place preferentially on the most energetic sites of the surface, which can be associated to positions in narrow pores or to the presence of active sites on the surface.

Table (4) : Parameters found from the fitting of the experimental results of adsorption of CTAB surfactants onto the activated carbon by simple and bi Langmuir equation.

| **Parameter** | **Value** |
|---|---|
| Xm mmol/g | 33.80235 |
| B l/mmol | 0.76207 |
| R | 0.98 |
| $\Delta G_{ads}$ Kj/mol | -26.4 |
| Am $nm^2$/molecule | 0.05 |
| $\Delta g_{ads}$ ($10^{-20}$ J $molecule^{-1}$) | -4.4 |
| Xm2 | 32.68906 |
| B2 | 0.98238 |
| Xm3 | 8.45077 |
| B3 | 0.53444 |
| R2 | 0.96 |
| $X_{m3}/X_{m3}+X_{m2}$ | 20% |
| $\Delta G_{ads2}$ Kj/mol | 27.02 |
| $\Delta G_{ads3}$ Kj/mol | 25.5 |
| $\Delta g_{ads2}$ ($10^{-20}$ J $molecule^{-1}$) | -4.5 |
| $\Delta g_{ads3}$ ($10^{-20}$ J $molecule^{-1}$) | -4.25 |
| Am2 $nm^2$/molecule | 0.05 |
| Am3 $nm^2$/molecule | 0.2 |
| $\Delta g_{adsmi}$ ($10^{-20}$ J $molecule^{-1}$) | -4.54 |

As in Table (4), there is a very good correlation in all systems between these two groups of results, analysis of Langmuir equation at concentrations below the c.m.c. and curve 3 from double Langmuir scheme, which suggests that the treatment of the experimental results with this scheme gives a good representation of the adsorption systems.

The second adsorption mechanism that can be assumed in our systems is that represented by curve 2 (Figures 1 – 4) and through $Am_2$ and $\Delta g_{ads2}$ values (Table 4). The $Am_2$ values are much lower that those corresponding to the process represented by curve 3 ($Am_3$). Bearing in mind that an important part of the BET-specific surface area of the adsorbent is not accessible to the CTAB molecules, these results reflect some arrangement of adsorbed molecules on the carbon surface, as adsorption progresses probably by the formation of surfactant aggregates in the adsorbed layer by interactions of the newly adsorbed molecules with those already fixed onto the solid surface.

This possibility of aggregate formation can be confirmed by the adsorption free energy. Since micellization takes place by the interactions of surfactants molecules through water, a measure of the interaction free energy of surfactant molecules in the aqueous phase can be obtained from their micellization free energy, $\Delta G_{mi}$. In aqueous solutions where the c.m.c. is lower than $10^{-1}$ mol $l^{-1}$, $\Delta G_{mi}$ can be calculated

according to [45] :

$$\Delta G_{mi} = RT \ln(c.m.c./\omega) \quad (5)$$

Taking into account the c.m.c. of surfactants at 20 $^{o}$C , the values per molecule, $\Delta G_{mi}$, obtained are -4.54 X $10^{-20}$ J molecule$^{-1}$. It can be seen that the values of $\Delta g_{ads2}$ are similar in absolute value of $\Delta G_{mi}$. However, the correlation between both values suggesting that the two interaction mechanisms are more similar. In accordance with the proposal that above the c.m.c., the adsorption mechanism of CTAB molecules takes place through interactions with those previously adsorbed, it is expected that the differences found in the first adsorption layer are also reflected on the second adsorbed layer. The CTAB molecules retained by direct interaction with the carbon surface have a configuration allowing a interaction between surfactant molecules more similar than that in micelles, and then decreasing the differences between $\Delta g_{ads2}$ and $\Delta G_{mi}$ values [42].

## Conclusion :

The current work focused on sorption of CTAB from aqueous solutions onto corncob-based activated carbon for a better understanding of the kinetics and equilibrium adsorption. The results present in this paper show CTAB was adsorbed by the exterior surface of AC particle at the beginning, so the adsorption rate was very fast. When the adsorption of the exterior surface reached saturation, the CTAB entered into PAC particle by the pore within the particle and was adsorbed by the interior surface of the particle.

Although intraparticle diffusion played a significant role, it was not the main rate determining step throughout the adsorption. Both intraparticle diffusion and boundary layer diffusion seem significant in the rate controlling step. A comparison of the kinetic models on the overall adsorption rate showed that CTAB/PAC system was best described by the pseudo second order rate model and sorption can not been described with first order model.

Based on our results, it can be concluded that the use of a double Langmuir scheme for the analysis of the studied adsorption system provides deeper information on the evolution of the retention process and the differences in the behavior of the surfactants selected.

## References :


[1] P. C. Pavan, E. L. Crepaldi, and J. B. Valim, J. Colloid Interface Sci. 229 (2000) 346.
[2] C. E. Hoeft, and R. L. Zollars, J. Colloid Interface Sci. 177 (1996) 171.
[3] N. Paxeus, Water Res. 30 (1996) 1115.
[4] P. C. Pavan, E. L. Crepaldi, G. A. Gomes, and J. B. Valim, Colloids Surf. 154 (1999) 399.
[5] R. A. Garcia-Delgado, L. M. Cotoruelo, and J. J. Rodriguez, Sep. Technol. 27 (1992) 1065.
[6] J. J. Kipling, "Adsorption from Solutions of Non-Electrolytes." Academic Press, London, 1965.
[7] A. K. Vanjara, and S. G. Dixit, Langmuir 11 (1995) 2504.
[8] J. F. Scamehorn, R. S. Schechter, and W. H. Wade, J. Colloid Interface Sci. 85 (1982) 463.
[9] H. Huang, and P. Somasundaran, Colloids Surf. A 117 (1996) 235.
[10] W. Brown, and J. Zhao, Macromolecules 26 (1993) 2711.
[11] I. Yoshio, and T. Suzawa, Bull. Chem. Soc. Jpn. 43 (1970) 3364.
[12] H. P. Boehm, Adv. Catalysis 16 (1966) 179.
[13] H. P. Boehm, Carbon 32 (1994) 759.
[14] T. Bandosz, Carbon 37 (1999) 483.
[15] I. I. Salame, and T. J. Bandosz, J. Colloid Interface Sci. 210 (1999) 367.
[16] A. R. Hind, S. K. Bhargava, and S. C. Grocott, Colloids Surf. A 146 (1999) 359.
[17] R. C. Bansal, J. B. Donnet, and F. Stoeckli, "Activated Carbon" Dekker, New York, 1988.
[18] J. Pastor-Villegas, C. J. Dur´an-Valle, C. Valenzuela-Calahorro, and V. G´omez-Serrano, Carbon 36 (1998) 1251.
[19] M. Smisek, and S. Cerny, "Activated Carbon." Elsevier, Amsterdam, 1970.
[20] T. Otowa, Y. Nojima, and T. Miyazaki, Carbon 35 (1997) 1315.
[21] T. J. Bandosz, J. Jagiello, C. Contescu, and J. A. Schwarz, Carbon 31 (1993) 1193.
[22] F. Rodriguez-Reinoso, and M. Molina-Sabio, Adv. Colloid Interface Sci. 76–77 (1998) 271.
[23] P. Pendleton, S. H. Wong, R. Schumann, G. Levay, R. Denoyel, and J. Rouquerol, Carbon 35 (1997) 1141.
[24] R. Considine, R. Denoyel, P. Pendleton, R. Schumann, and S. Wong, Colloids Surf. A 179 (2001) 271.
[25] A. B. Qing Cao, K. C. Xie, Y. K. Lv, W. R. Bao, Bioresource Technology 97 (2006) 110.
[26] H. Marsh and B. Rand, J. Colloid Interface Sci. 33 (1970) 101.
[27] G. D. Halsey, J. Chem. Phys. 16 (1948) 931.
[28] M. J. Rosen, Surfactants and Interfacial Phenomena, New York : Wiley; 1978.
[29] S. Brunauer, L. S. Deming, W. S. Dening, and E. Teller, J. Am. Chem. Soc. 62 (1940) 1723.
[30] Y. P. Guo, S. F. Yang, J. Z. Zhao, Z. C. Wang, M. Y. Zhao, Chemical Journal of Chinese Universities 21/3 (2000) 335.
[31] H. Marsh and B. Rand, J. Colloid Interface Sci. 33 (1970) 101.
[32] M. Özacar and I. A. Sengil, Bioresource. Tech. 96 (2005) 791.
[33] Y. S. Ho, and G. McKay, Process Biochem. 34 (1999) 451.
[34] R. S. Juang, F.C. Wu, and R. L. Tseng, J. Colloid. Interf. Sci. 227 (2000) 437.
[35] W. J. Weber, J. C. Morris, and J. Sanit, Eng. Div. Am. Soc. Civ. Eng. 89/SA2 (1963) 31.
[36] M. Basibuyuk, and C. F. Forster, Process Biochem, 38 (2003) 1311.
[37] MEHMET YALC, IN AND AHMET G¨ URSES, C, ETIN DO ¢ GAR, MUSTAFA S ¨ OZBÿILÿIR The

Adsorption Kinetics of Cethyltrimethylammonium Bromide (CTAB) onto Powdered Active Carbon Adsorption 10: (2004) 339–348.
[38] P. Santanu, K. C. Khilar, Advances in Colloid and Interface Science 110 (2004) 75.
[39] A. Upadhyaya, E. J. Acosta, J. F. Scamehorn, D. A. Sabatini, J Surfact. Deterg. (2007) 10:269–277 DOI 10.1007/s11743-007-1045-3.
[40] P. Punyapalakula, S. Takizawab, Water Research 40 (2006) 3177 – 3184.
[41] S. Natasja, G. J. Louis, van der Hamb, G. Jan, W. Euverinka, Andre´ B. de Haanc, Water Research 41 (2007) 4233.
[42] C. M. Gonza´lez-Garc´, M. L. Gonza´lez-Mart´n, J. F. Gonza´leza, E. Sabioa, A. Ramiroa, J. Gana´na, Powder Technology 148 (2004) 32.
[43] Erik Kissa, Fluorinated Surfactants and Repellents, Published by CRC Press, 2001 ISBN 082470472X, 9780824704728 615 pages
[44] Y. Yang, Y. Chun, G. Sheng, M. Huang, Langmuir 20 (2004) 6736.
[45] M. J. Rosen, Surfactant and Interfacial Phenomena, Wiley Interscience, New York, 1989, pp. 108–169.